

# **Adaptive Intelligent Combustion Control Based on Data-Driven Low-Order Models**

**Tongxun Yi  
Domenic Santavicca  
Penn State University**

**Presented at the 2009 NASA Propulsion Control and Diagnostics Workshop  
Cleveland Airport Marriott Hotel, Cleveland, Ohio  
December 8 – 10, 2009**



**\*NASA Award No: NNX07C98A**

# Content

- 1. Why Data-Driven Model-Based Combustion Control**
- 2. Fuel Modulation Techniques**
- 3. Combustion Sensing Techniques**
- 4. Flame Transfer Functions and Control Design Perspective**
- 5. Conclusions and Suggested Future Work**
- 6. Reference**

# 1. Why Data-Driven Model-Based Combustion Control



NASA Award No: NNX07C98A

# Necessity of Advanced Combustion Control

For gas turbine combustors, the design strategies favoring different performance indices are usually not compatible. Combustion control adds extra freedom to improve and optimize overall performance. A typical example is developing control systems to enhance lean combustion stability so that the engines can operate in clean, safe, and stable manner.

- Three adaptive phase-shift controllers (Gatech, UTRC, and Yi&Gutmark). The last one is capable of identifying the dominant frequency within one pressure cycle and a half, with an estimation error within 5 Hz, and is free of stability concerns
- Mixed control performance has been reported, including insufficient suppression of slightly-damped modes. These are the intrinsic deficiencies of phase-shift control principles.
- Model-based control design is a standard routine for control engineers and theorists. Data-driven models are in particular attractive and practical.
- Enough evidence suggests that model-based controllers can easily outperform the empirical ones, and for highly nonlinear systems, a simple nonlinear controller can well outperform linear ones.

***No knowledge can be certain if it is not based on mathematics.***

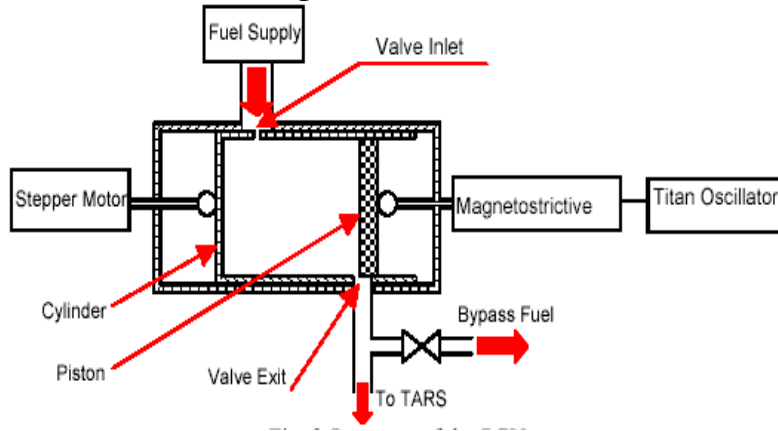
(Leonardo da Vinci)



# Example 1. Empirical Vs. Model-based Control

## Mean Flow Control of the Goodrich Valve: PD Vs. LQG Control

Goodrich Magnetostrictive Valve



System Identification Model

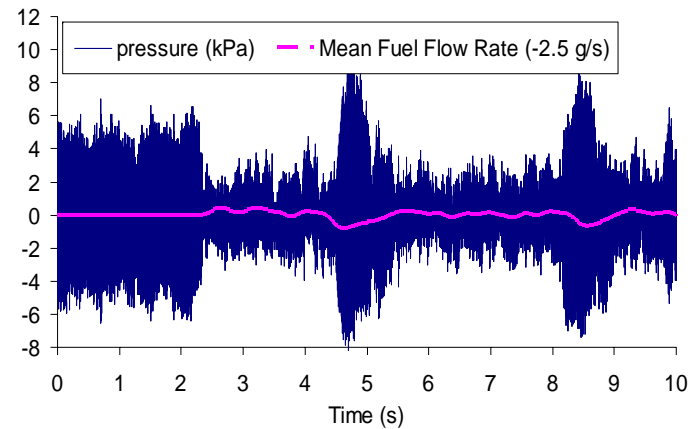
$$\frac{\dot{M}_0}{U(s)} = -\frac{0.004198s^3 - 1389s^2 - 6.284E6s - 6.431E10}{s^4 + 7287s^3 + 4.155E7s^2 + 2.744E11s + 3.033E9}$$

$$\dot{X} = A_c X + Gy$$

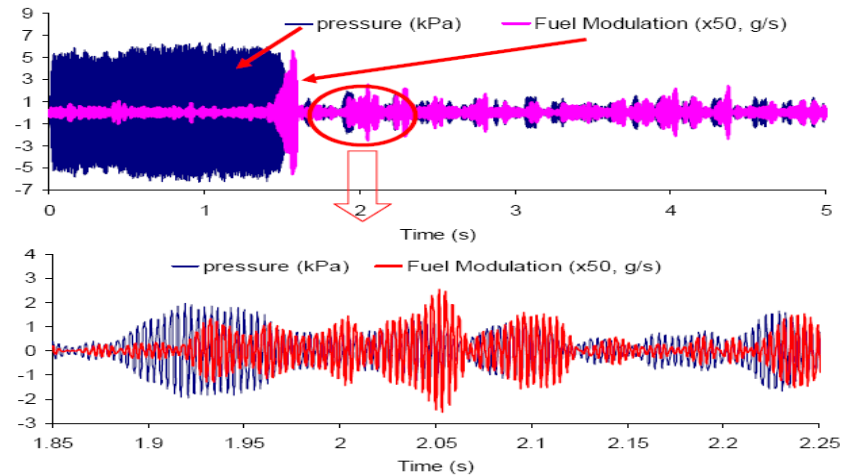
$$u = -B^T X$$

$$G = 0.001 \begin{pmatrix} 0.3067 \\ 0.005 \\ -0.0027 \\ -0.0013 \end{pmatrix}; B = 1000 \begin{pmatrix} -7.0633 \\ -3.3158 \\ 8.3638 \\ 3.4277 \end{pmatrix}$$

PD Control of Mean Flow

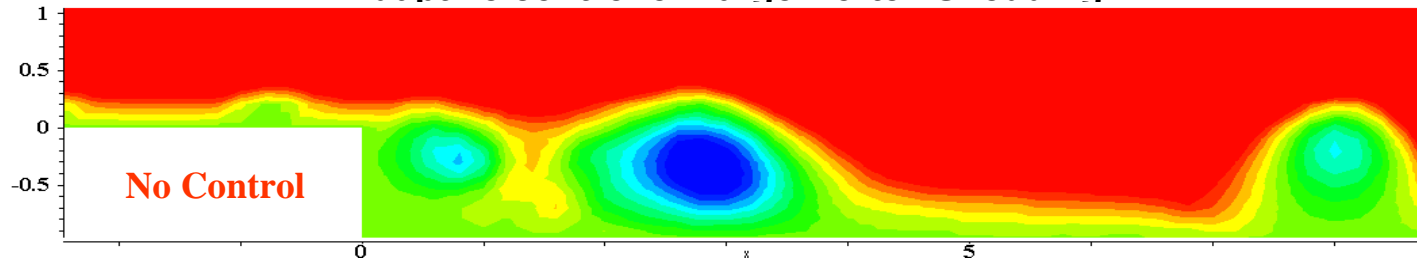


LQG Control of Mean Flow



# Example 2. Linear Vs. Nonlinear Control

Adaptive control of Large-Vortex Shedding



N-S Equation: 
$$\frac{D\bar{U}}{Dt} = -\nabla p + \frac{1}{Re} \Delta \bar{U}; \nabla \cdot \bar{U} = 0$$

POD-based Model: 
$$\bar{U}(\bar{S}, t) = \bar{U}_0(\bar{S}, t) + \sum_{i=1}^{\infty} x_i(t) \Phi_i(\bar{S})$$

$$\Rightarrow \begin{cases} \dot{X}_{N \times 1} = A_{N \times N} X + X^T B_{N \times N \times N} X + D_{N \times 1} \\ X(0) = X_0 \end{cases}$$

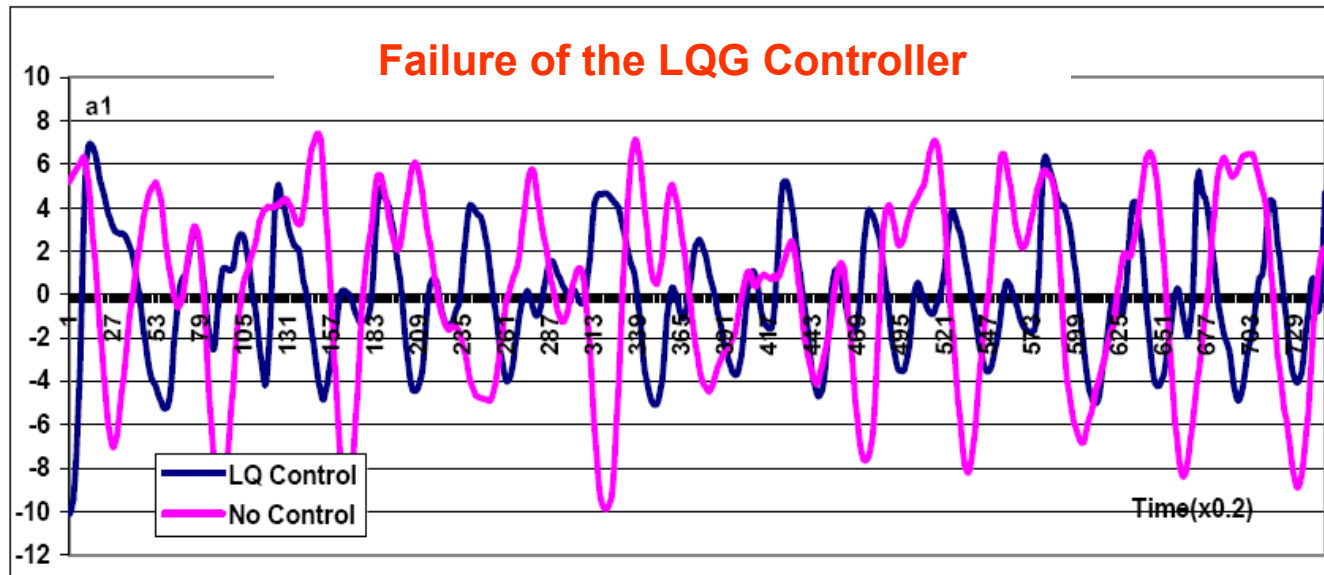


Figure 1. The first POD mode-coefficient  $a_1(t)$  with and without the LQ-controller.

# Example 2. Linear Vs. Nonlinear Control (cont.)

## SISI Reduced-Order Model

$$\mathbf{a}_1 \dot{\mathbf{x}} + \mathbf{a}_2 \mathbf{x} + \mathbf{a}_3 \mathbf{x}^2 + \mathbf{a}_4 + \mathbf{e} = \mathbf{u}$$

$a_1, a_2, a_3$  and  $a_4$ : constant or slow-varying but unknown ( $a_1 > 0$ );  
 $e$ : bounded unmodeled dynamics and external disturbance,

## Adaptive control Law

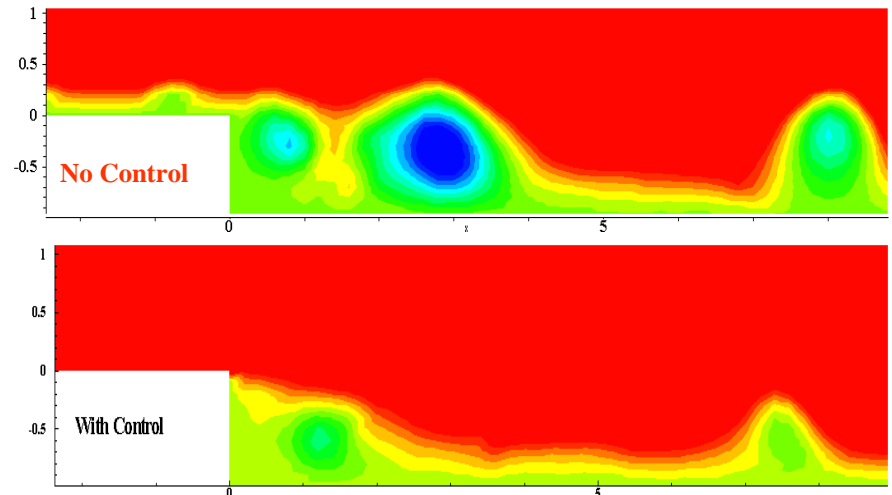
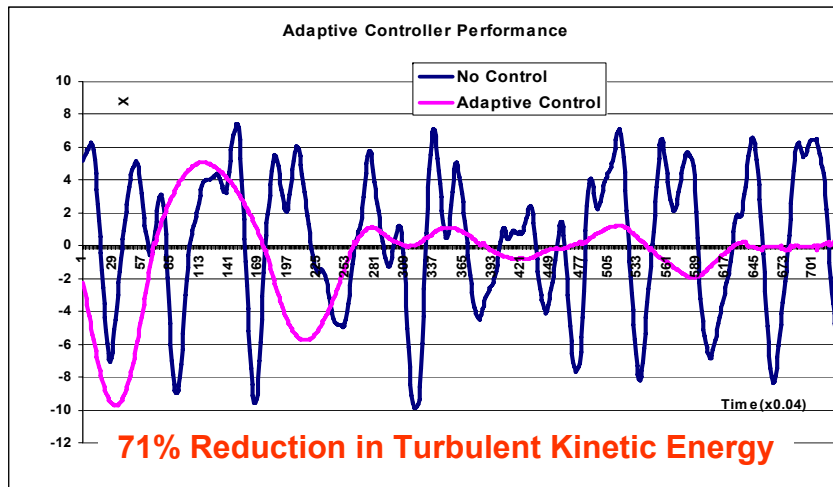
$$\mathbf{u} = \mathbf{Y}^T \hat{\mathbf{A}} - k s; s = \mathbf{x} - \mathbf{x}_d; \dot{\hat{\mathbf{A}}} = -\Gamma \mathbf{Y} s_\Delta; s_\Delta = s - \Phi \text{sat}\left(\frac{s}{\Phi}\right); \Phi = \frac{E}{k}$$

## Stability Proof

$$V = \frac{1}{2} a_1 s_\Delta^2 + \frac{1}{2} \tilde{\mathbf{A}}^T \Gamma^{-1} \tilde{\mathbf{A}}; \dot{V} = s_\Delta (u - \mathbf{Y}^T \mathbf{A} - e) - \dot{\hat{\mathbf{A}}}^T \Gamma^{-1} \tilde{\mathbf{A}}$$

$$= -k s_\Delta^2 - (s_\Delta \mathbf{Y}^T + \dot{\hat{\mathbf{A}}}^T \Gamma^{-1}) \tilde{\mathbf{A}} - s_\Delta [k \Phi \text{sat}\left(\frac{s}{\Phi}\right) - e] \leq -k s_\Delta^2$$

$\ddot{V}$  is bounded, so global stability is guaranteed (Barbalat's Lemma).

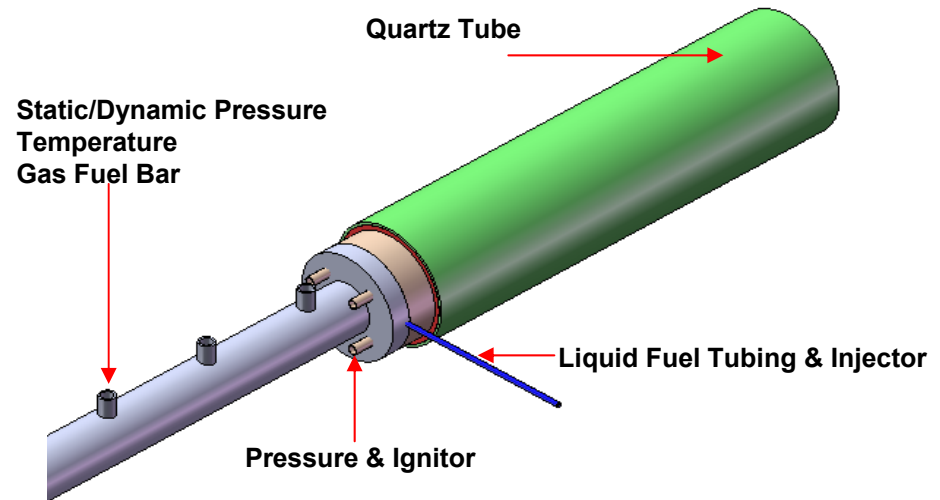
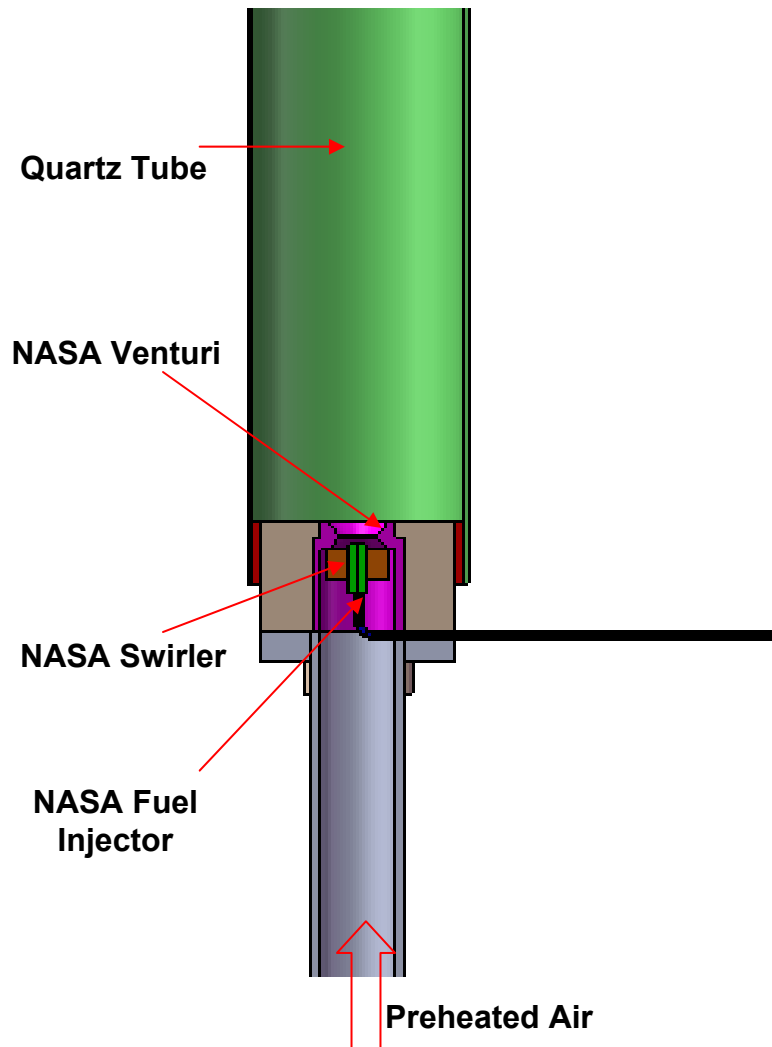


## 2. Fuel Modulation Techniques



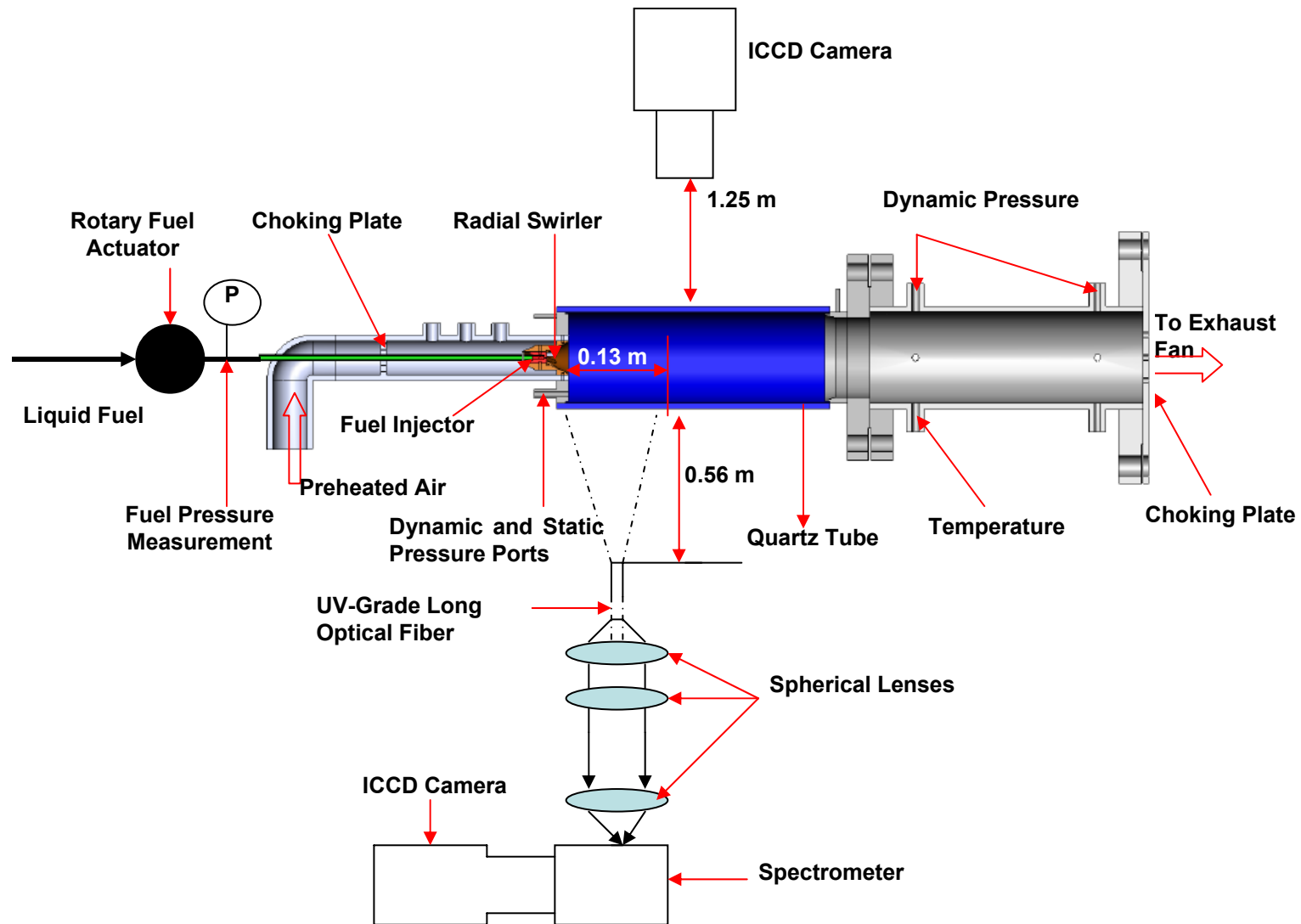
NASA Award No: NNX07C98A

# The NASA Combustion Rig

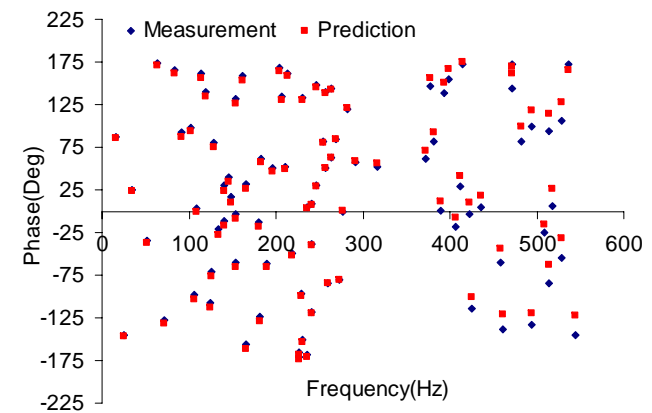
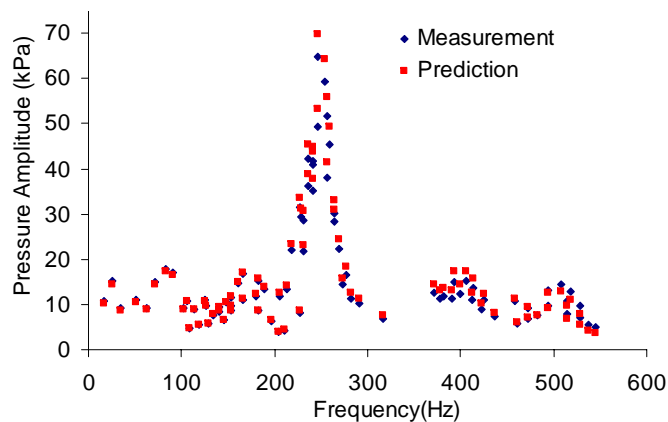
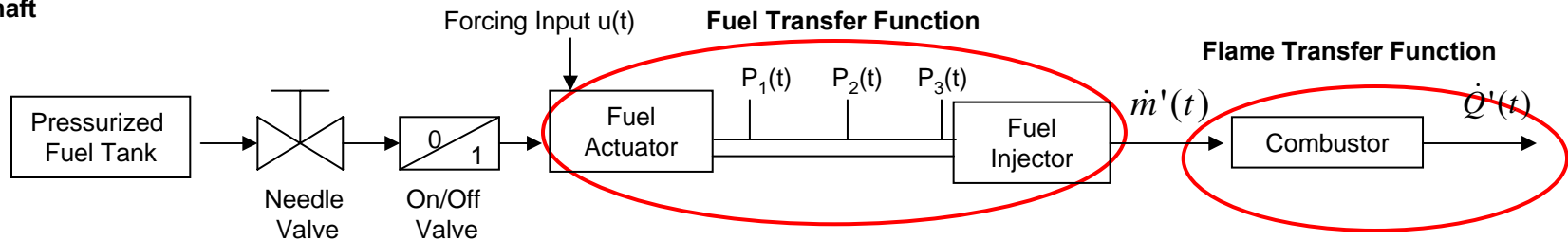
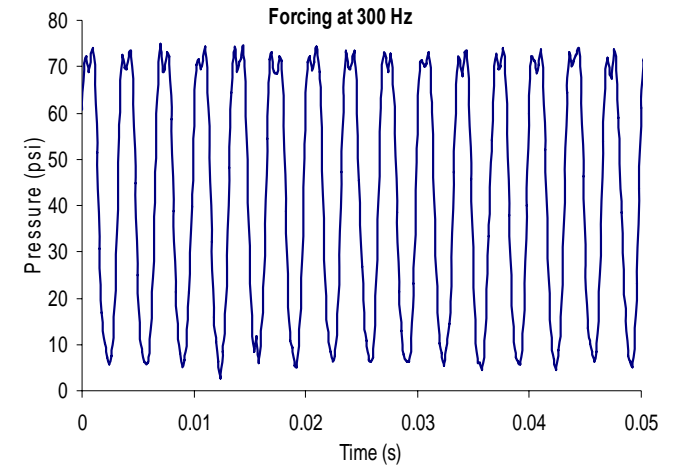
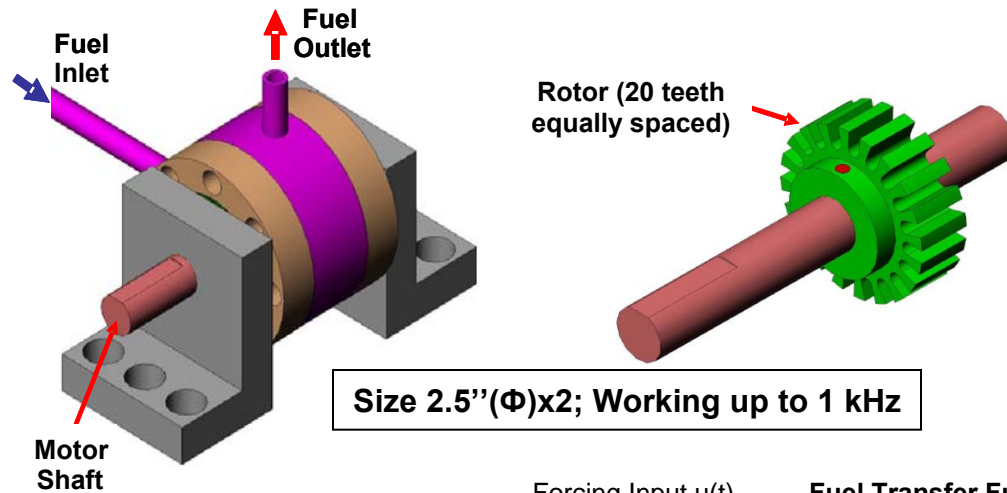


- Visually-observed axisymmetric flame
- Pressure drop within 4% up to 70 SCFM
- Nice blue flame below  $\Phi=0.38$
- Somewhat red/yellow flame above  $\Phi=0.38$
- Jet-like flow with vortex breakdown, not easy to ignite
- Comparable LBO limits with the previous one
- Comparable air pressure drop with the previous one
- Large fuel pressure drop, about 4 times larger
- Less efficient fuel/air mixing than the previous one which has no red/yellow flame up to  $\Phi=0.60$

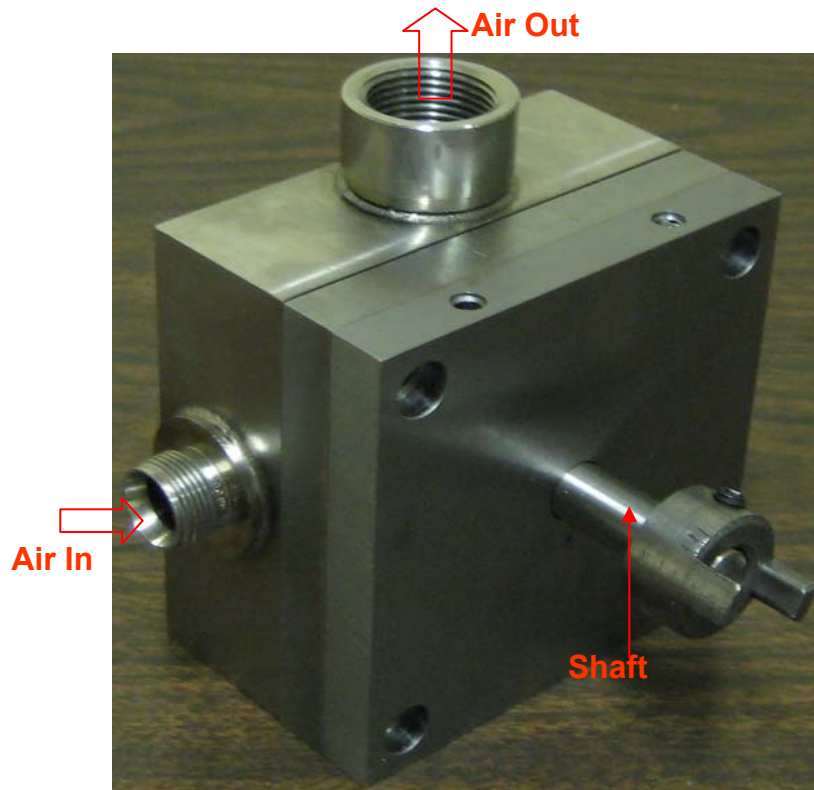
# Experiment Setup



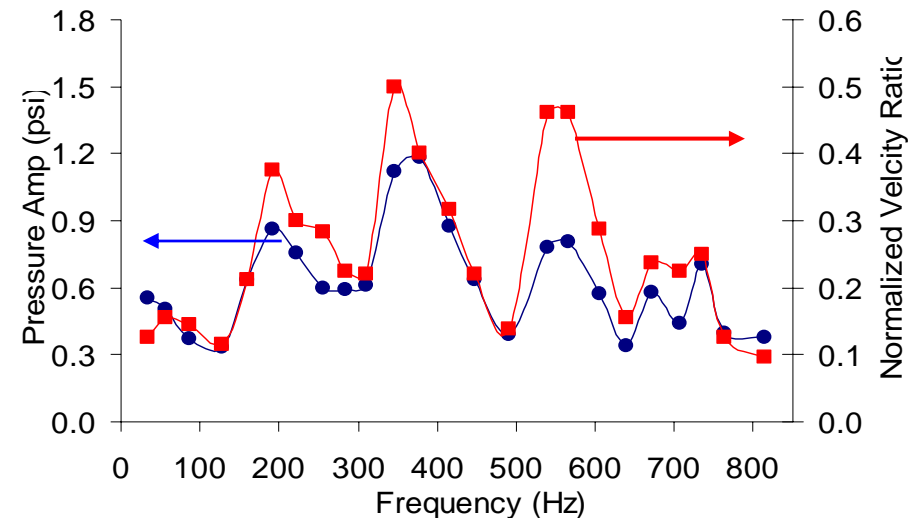
# Motor-Driven High-Frequency Fuel Valve



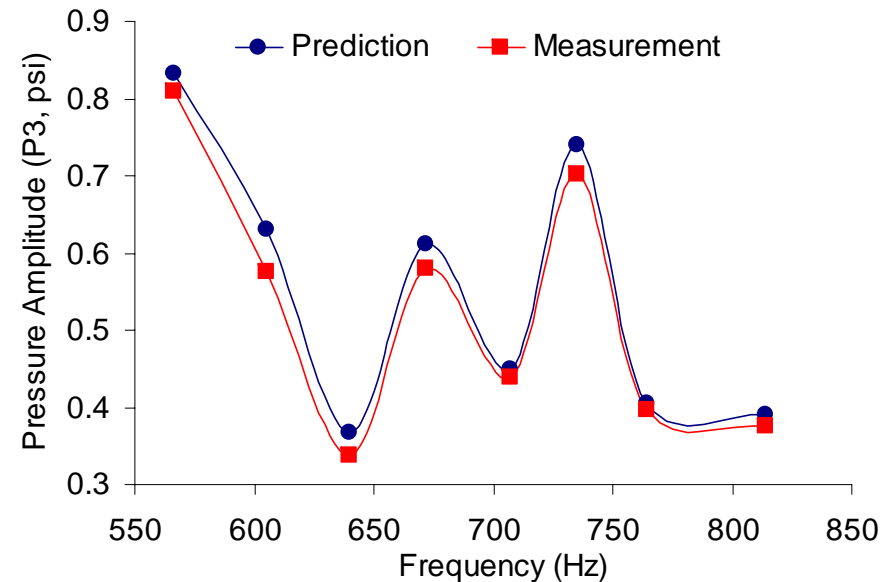
# Motor-Driven High-Frequency Air Valve



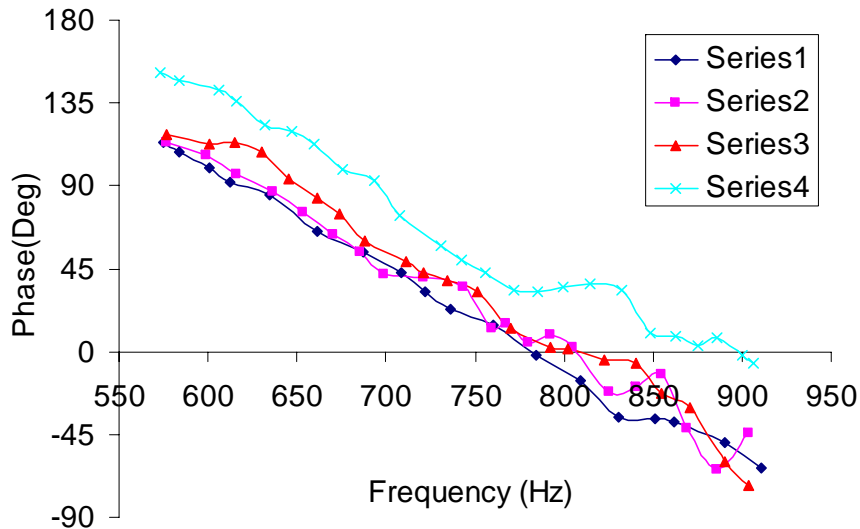
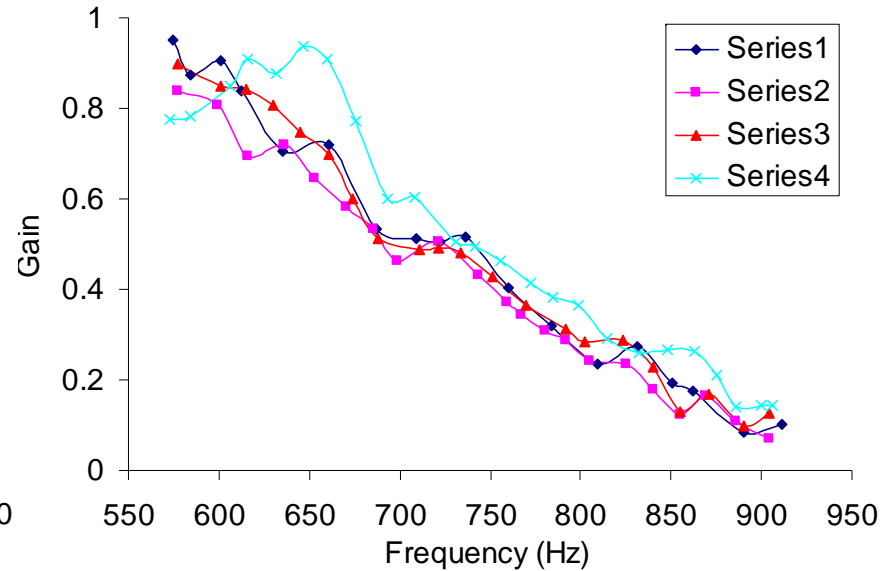
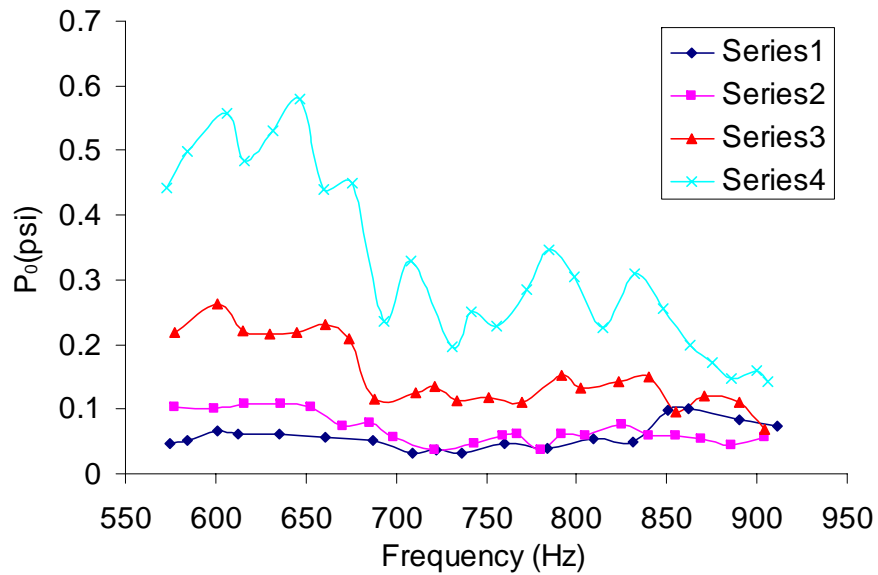
- Driven by a variable speed DC motor
- Modulation frequency up to 900 Hz
- Inlet velocity modulations above 50% up to 800 Hz
- Size 4"x4"x2.5"



## Air Flow 60 SCFM



# Flame Response to Air Modulations



**Air: 40 SCFM; Preheat Temperature: 373 K**

**Flame Transfer Function:**  $G(s) = \frac{CH^*(s)}{P_0(s)}$

**Air modulations above 900 Hz**

**Nonlinearity in terms of the forcing amplitude, in particular around the one-wave resonant frequency**

**Quite some details need to be figured out**

# 3. Combustion Sensing Techniques



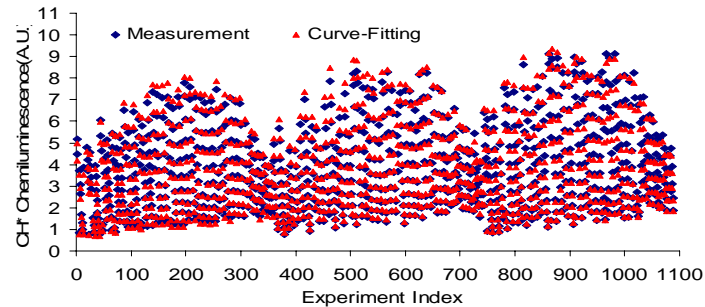
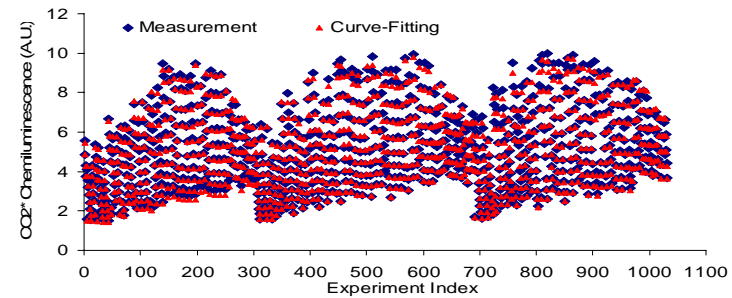
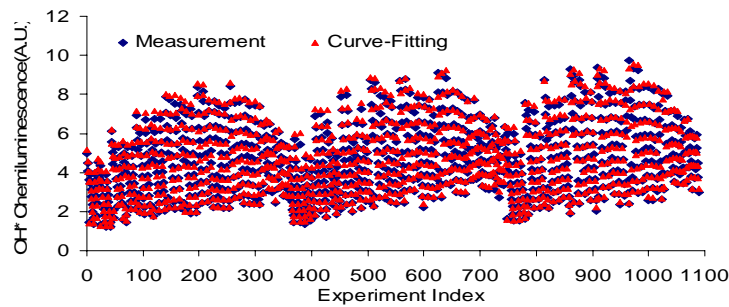
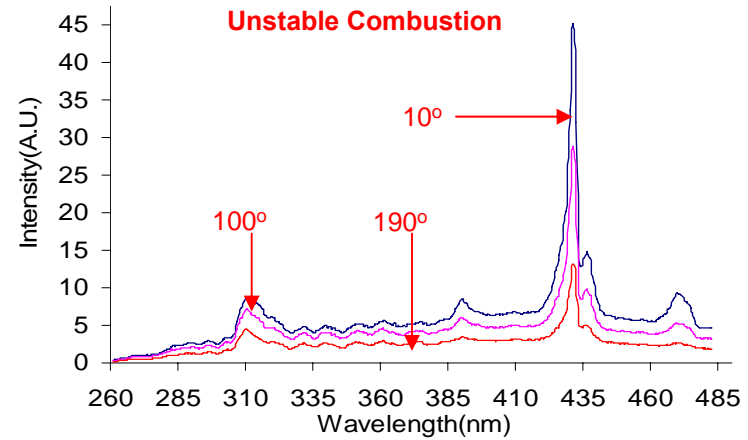
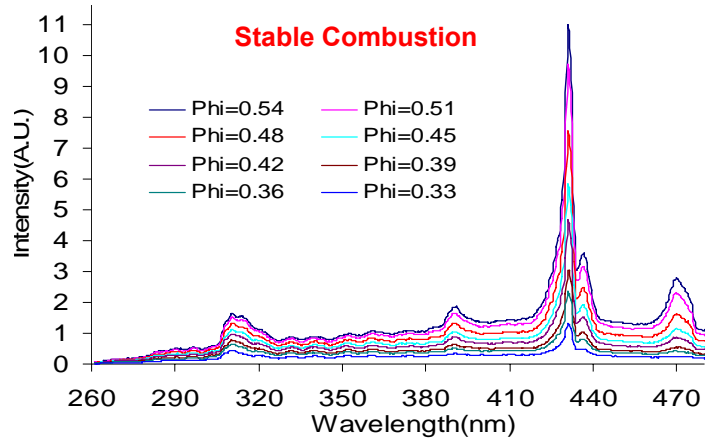
NASA Award No: NNX07C98A

# Background of Combustion Sensing

- The instantaneous heat release rate and equivalence ratios are two key parameters for combustion analysis and control. Chemiluminescence-based sensors are practical solutions.
- For premixed gas-fueled combustion, linearity between chemiluminescence yield and heat release is valid for slightly turbulent or wrinkled flamelet region. But in the corrugated and broken flamelet region, nonlinearity cannot be ignored.
- In combustion instability analysis, it is usually assumed that chemiluminescence is proportional to the instantaneous heat release rate, which in fact, suffers from several major deficiencies.
- Reported is an accurate correlation-function-based method for real-time combustion sensing, based on chemiluminescence measurements using PMTs. For the first time in combustion literature, the nonlinearity among heat release, chemiluminescence, equivalence ratios, and acoustics effects is taken into account



# UV and VIS Flame Spectra



$$I_{307 \text{ nm}} = 94.61 \tilde{m}_a^{1.7558} \phi^{2.1369} \left( \phi + \frac{T_i}{2000} \right)^{1.1060} \tilde{p}^{-0.4522}$$

$$I_{365 \text{ nm}} = 115.85 \tilde{m}_a^{1.3637} \phi^{2.2280} \left( \phi + \frac{T_i}{2000} \right)^{0.8217} \tilde{p}^{-0.2183}$$

$$I_{430 \text{ nm}} = 212.05 \tilde{m}_a^{1.6627} \phi^{3.0735} \left( \phi + \frac{T_i}{2000} \right)^{1.4352} \tilde{p}^{-0.4045}$$

**Average Error: 2.4% for OH\* ; 2.0% for CO<sub>2</sub>\* ; 3.8% for CH\*.**



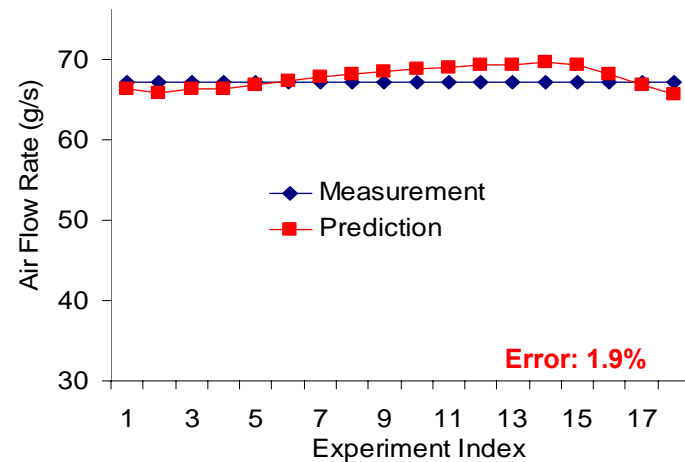
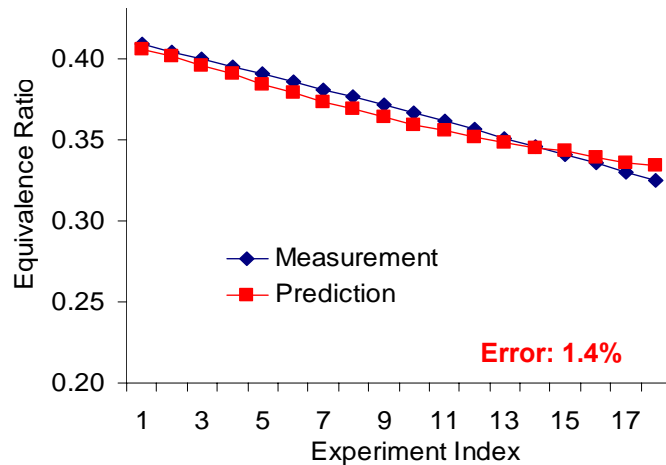
**NASA Award No: NNX07C98A**

# Combustion Sensing Strategy

The above correlation functions are mostly developed from stable combustion, thus they can be used to determine the mean heat release rate and the mean equivalence ratio (See JPP, Vol.129, No.5).

$$\begin{aligned} \tilde{m}(t) &= 0.1571(I_{307nm}(t))^{1.4747} (I_{365nm}(t))^{0.7294} (I_{430nm}(t))^{-1.5540} (\tilde{p}(t))^{0.1974} \\ \phi(t) &= 0.1392(I_{307nm}(t))^{-1.2966} (I_{365nm}(t))^{1.4942} (I_{430nm}(t))^{0.1437} (\tilde{p}(t))^{-0.2021} \\ \dot{Q}_R(t) &= 0.1\Delta H_R \tilde{m}(t)\phi(t) \left( \frac{\bar{m}_f}{\bar{m}_a} \right)_{stoichiometry} = 0.00674\Delta H_R \tilde{m}(t)\phi(t) = 281.7\tilde{m}(t)\phi(t)(kW) \end{aligned}$$

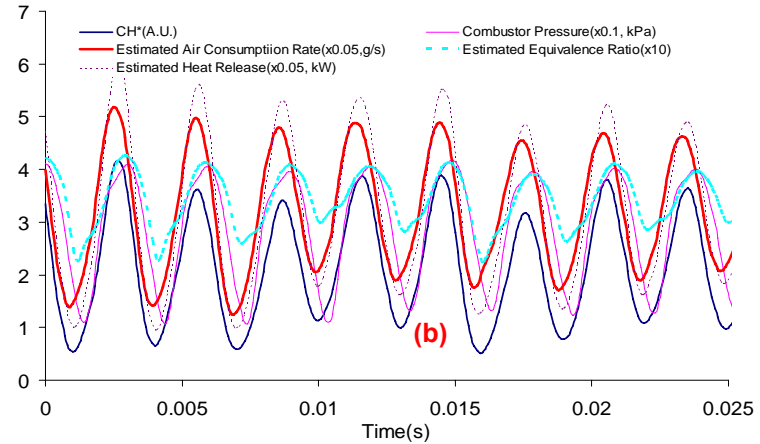
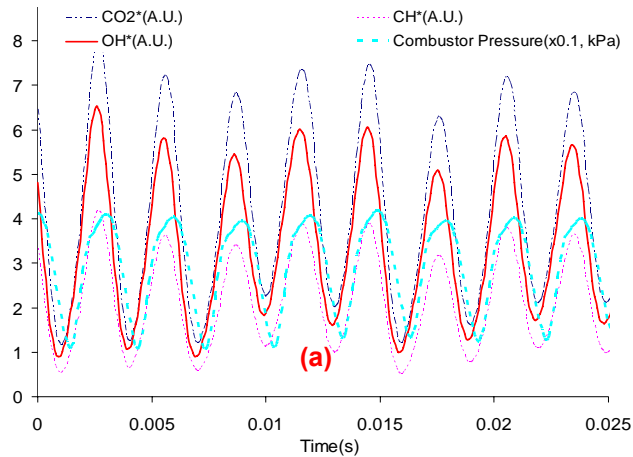
They are obtained by eliminating the term of flame temperature from the three correlation functions.



The estimated mean air consumption rate and the mean equivalence ratio. The air flow rate is 66.7g/s, the preheat temperature is 373 K, and the equivalence ratio is decreased from 0.41 to 0.31.

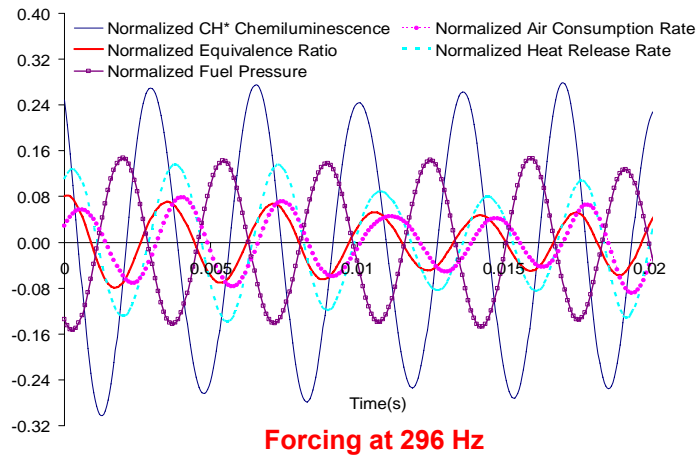
# Combustion Sensing Strategy (Cont.)

## Self-Excited Combustion Oscillations

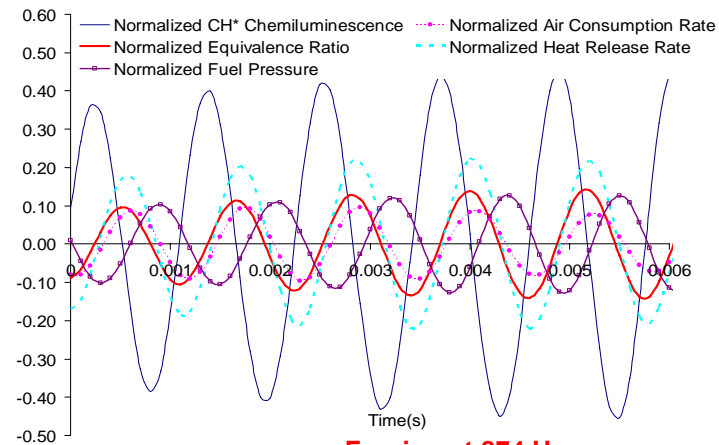


(a) Time traces of chemiluminescence and combustor pressure; (b) The estimated instantaneous air consumption rate, the estimated instantaneous equivalence ratio, and the estimated instantaneous heat release rate.

## Fuel Forcing Induced Combustion Oscillations



Forcing at 296 Hz



Forcing at 874 Hz

# 4. Flame Transfer Functions and Control Design Perspective

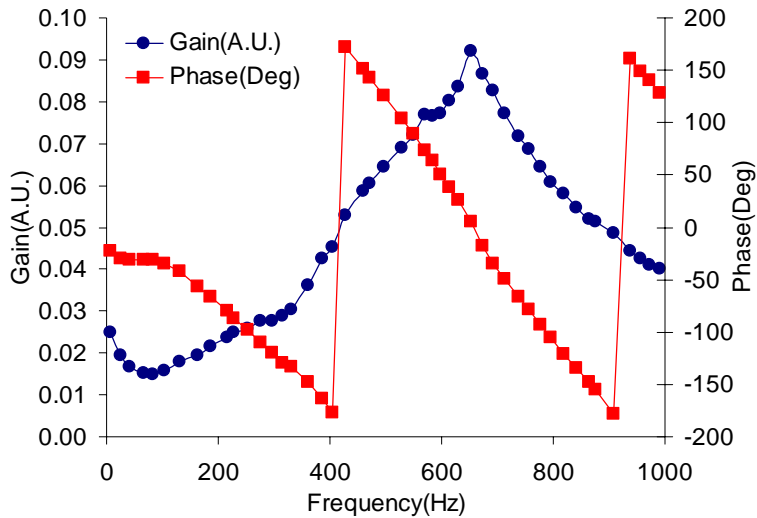


NASA Award No: NNX07C98A

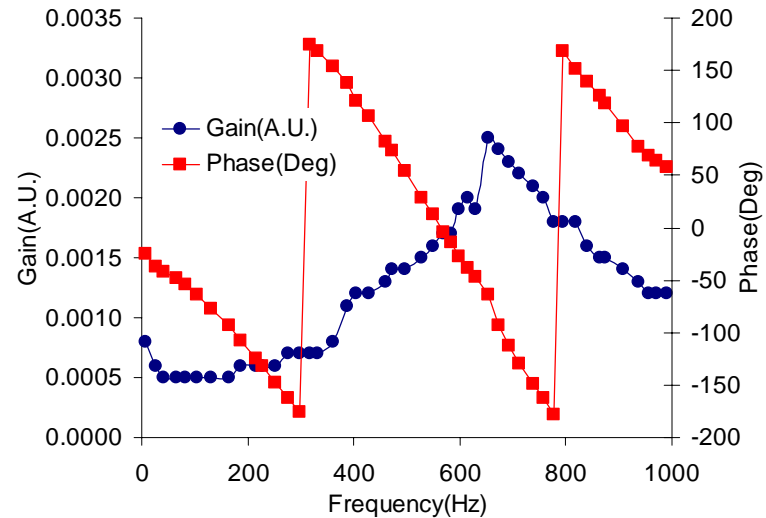
# Background

- **Combustion instability and lean blowout are major technical challenges for liquid-fueled DLE combustion. Both phenomena can be attributed to the increased sensitivity in heat release to external disturbances or intrinsic acoustic oscillations at very lean conditions.**
- **First-principle low-order modeling is challenging. The measured flame transfer functions (FTFs), i.e. heat release responses to inlet air and/or fuel modulations, provides an accurate description of combustion dynamics around the working conditions where they are derived.**
- **Active control of both phenomena can be achieved using small-amplitude fuel modulations, employing the same control hardware and fuel actuators. However, major differences exist.**
- **Acoustic responses are system- and geometry-dependent, but heat-release-based open-loop FTFs can be used for different types of engines employing the same type of burners.**

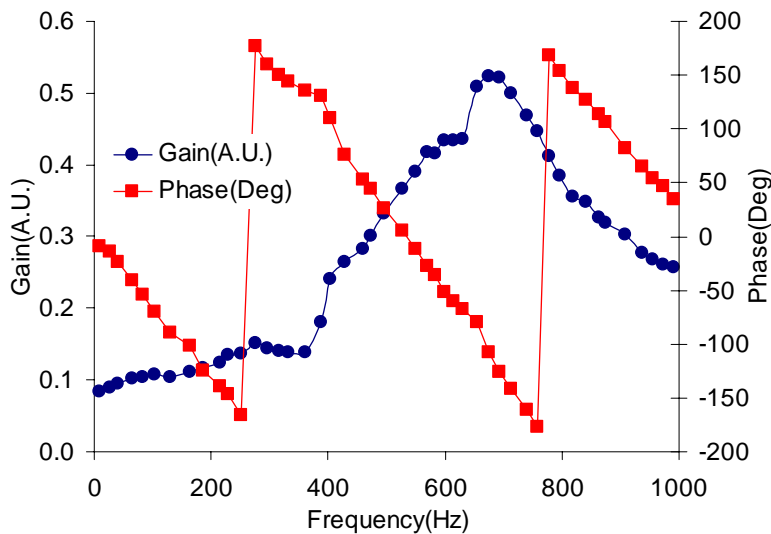
# Flame Transfer Functions



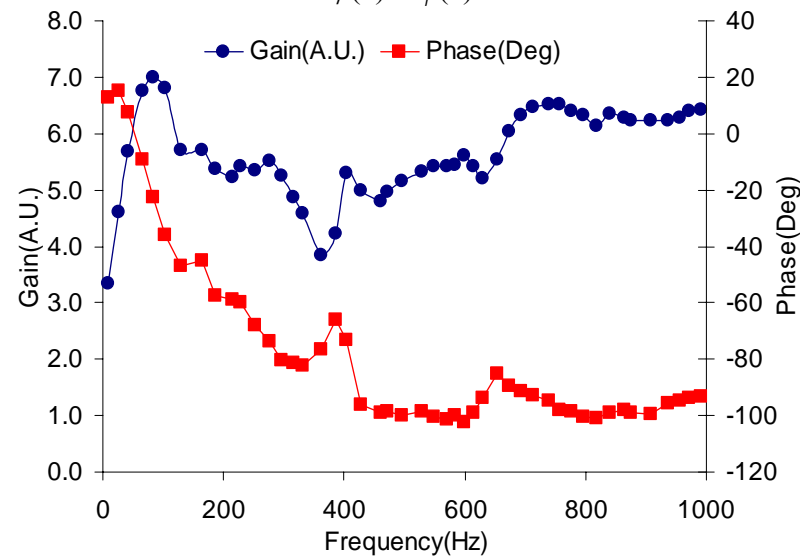
$CH^*(s)/P_f(s)$



$\phi(s)/P_f(s)$



$\dot{Q}_R(s)/P_f(s)$

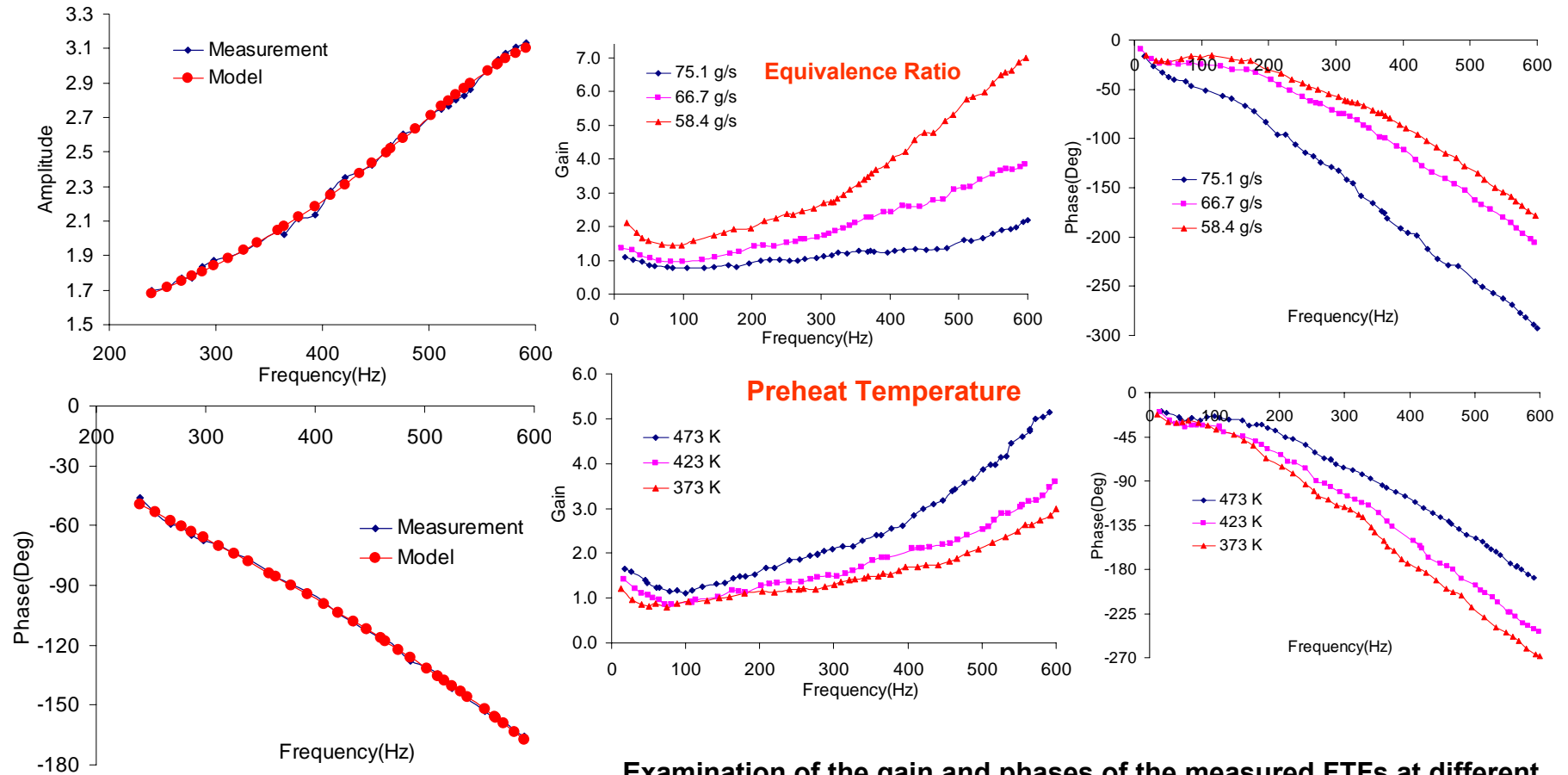


$\dot{Q}_R(s)/CH^*(s)$



# Control-Oriented Low-Order Modeling

The measured flame transfer function provides an accurate description of combustion dynamics.



$$W(z^{-1}) = \frac{CH^*(z^{-1})}{P_0(z^{-1})} = \frac{-0.4213z^{-2} + 1.604z^{-3} - 1.147z^{-4}}{1 - 1.952z^{-1} + 1.525z^{-2} - 0.5222z^{-3}}$$

Examination of the gain and phases of the measured FTFs at different working conditions sheds insight on adaptive robust control design.

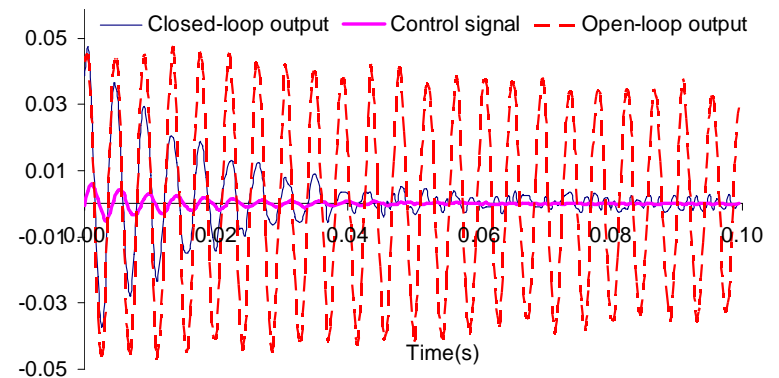
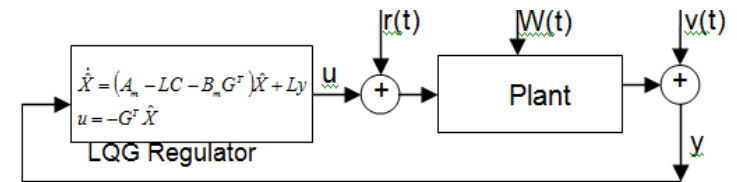
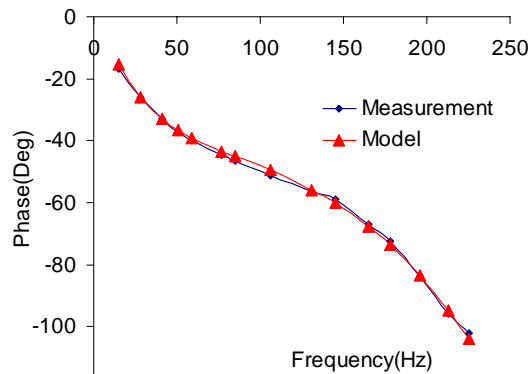
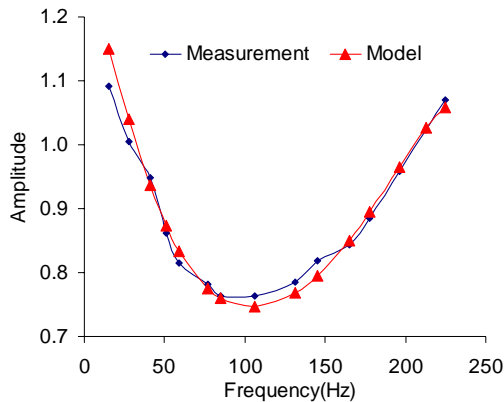


# Fast Control of LBO

LBO limits can be extended by increasing the amount of pilot fuel. But this approach is too slow, not suitable for transient LBO. In addition, locally hot regions form and exacerbate emissions.

Small-amplitude fuel modulations, based on a feedback controller, are capable of quickly attenuating small deviations from the equilibrium points within a small fraction of a second. Also detection of incipient LBO is not needed. The spatial fuel distribution is not modified, thus favoring low emissions.

Near-LBO combustion dynamics is rather slow, typically below 200 Hz. Thus the requirements of the actuator bandwidth and challenges associated with time delay are no longer major technical challenges.

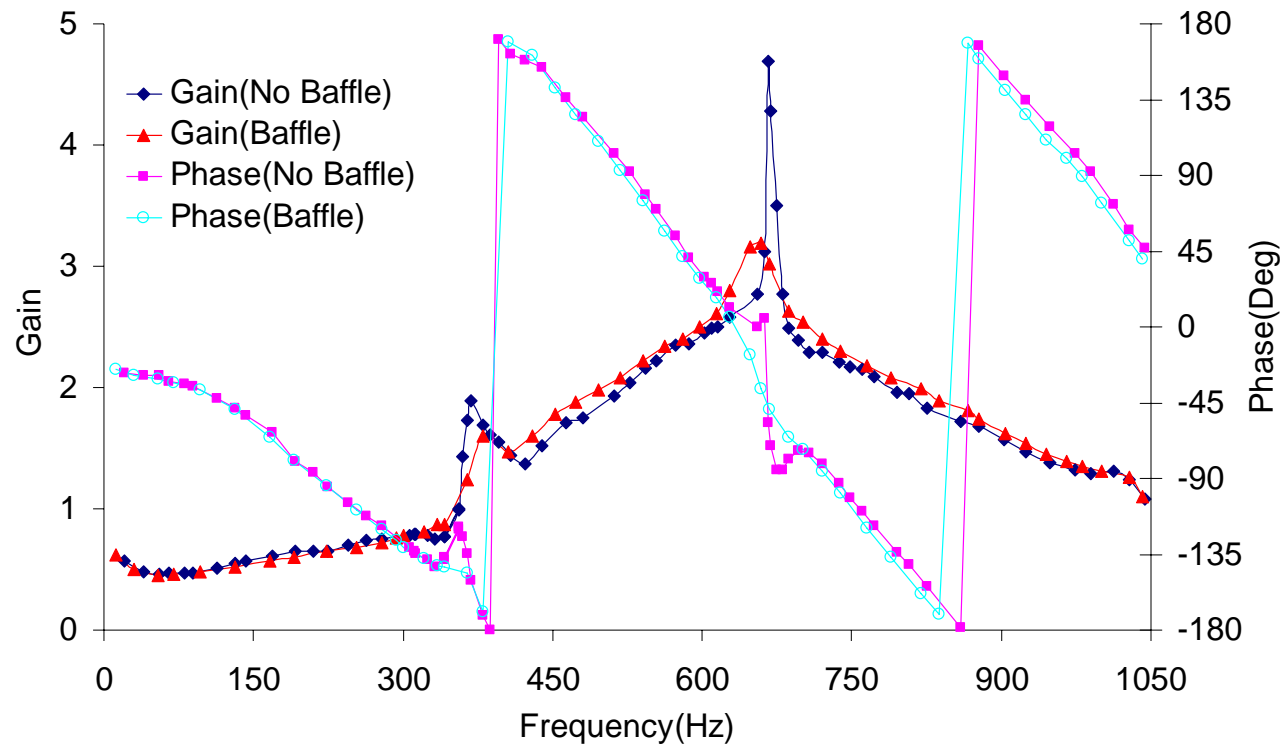


$$W(s) = \frac{37.2618(s+9793)(s+1262)}{(s+26.7)(s^2 + 6.6s + 2.119e6)}$$



# FTFs around Resonant Frequencies

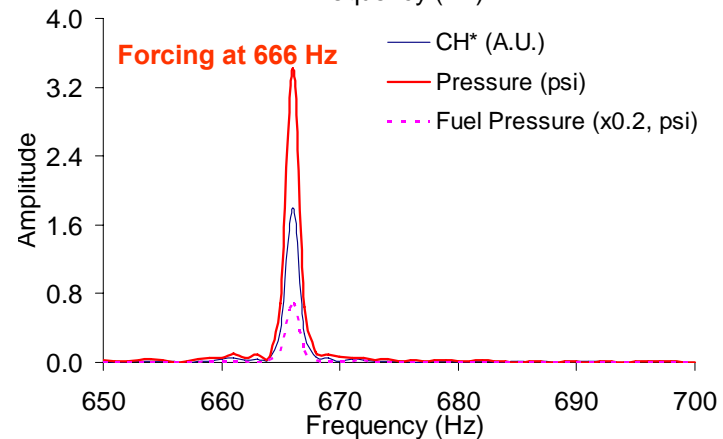
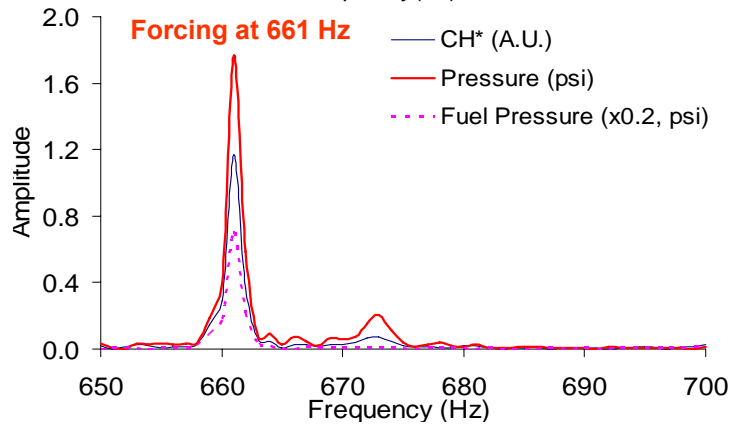
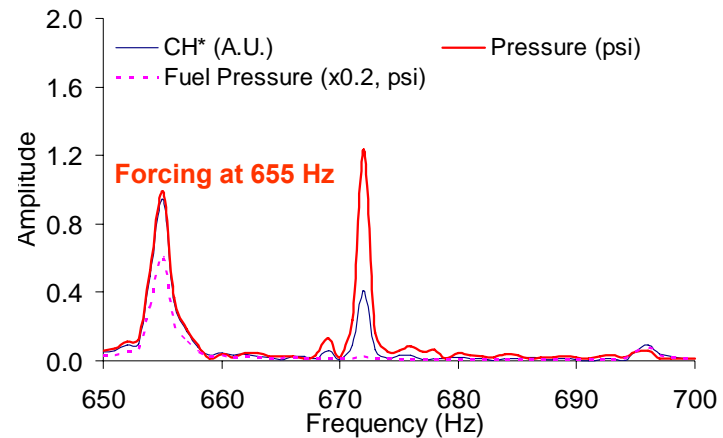
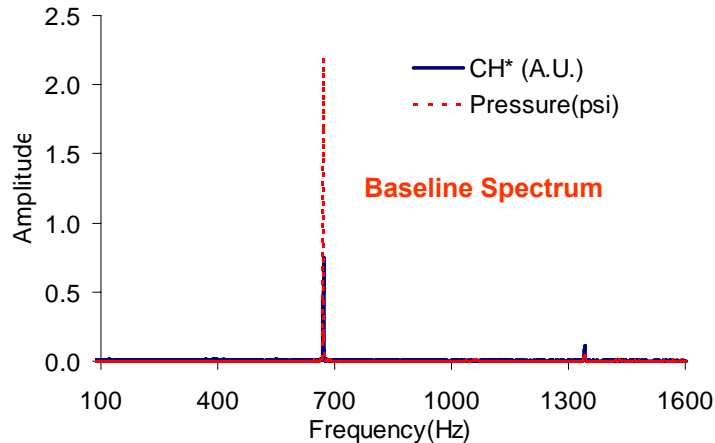
The FTFs around the acoustic resonant frequencies are no longer open-loop and linear. In this figure, off the resonant frequencies, i.e. around 340 Hz and 670 Hz, differences in both the gain and phases are rather small. Considerable differences exist around the acoustic resonant frequencies.



$\Phi=0.40$  , the air flow rate of 44.5 g/s, and  $T_i=373$  K. Stable combustion is achieved by inserting three baffle plates inside the combustion chamber.

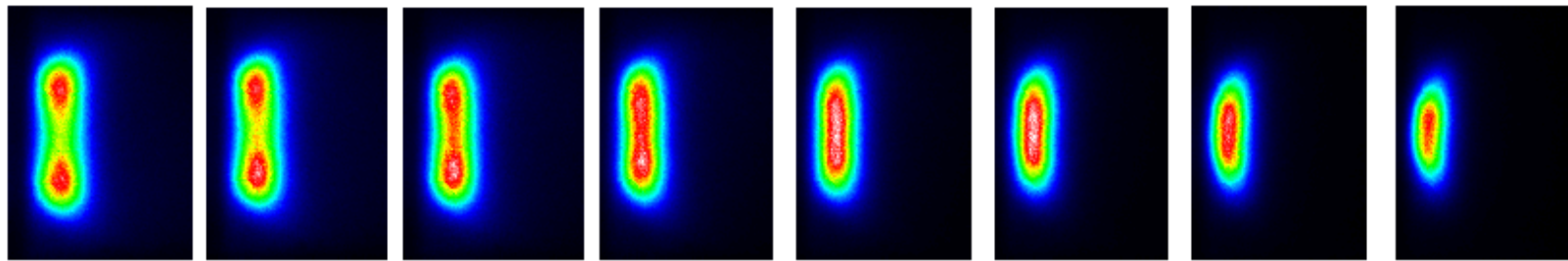
# Nonlinear Responses of Combustion Instability

Shown here are the quenching and entrainment of self-excited combustion instability with fuel modulation approaching the unstable frequency.

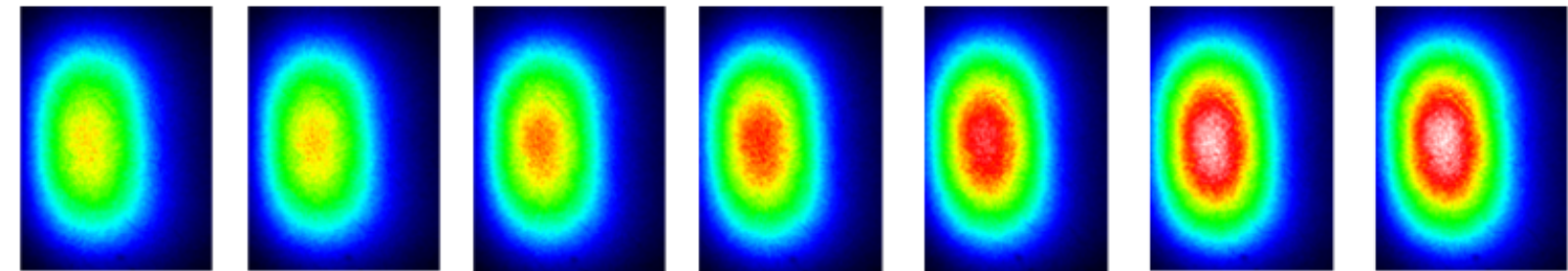
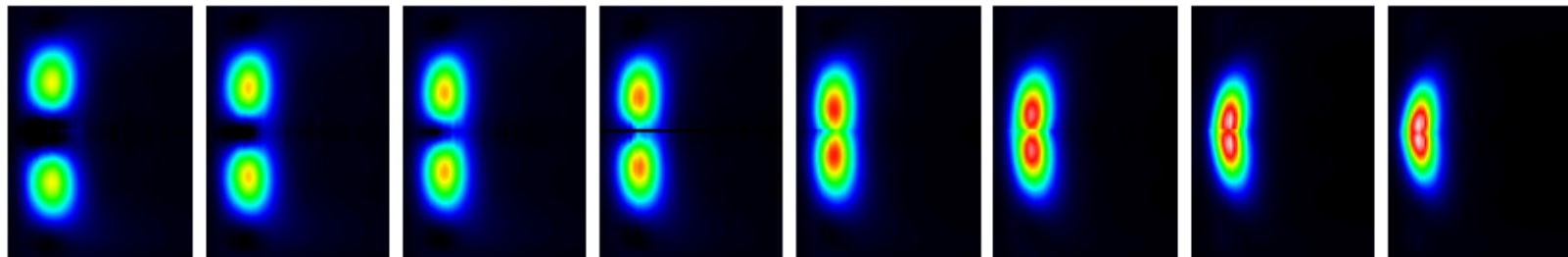


Unstable combustion occurs at  $\Phi=0.40$ , the air flow rate of 44.5 g/s, and  $T_i=373$  K. The fundamental resonant frequency is 672 Hz, corresponding to one-wave mode of the combustion chamber, 1.05-m-long.

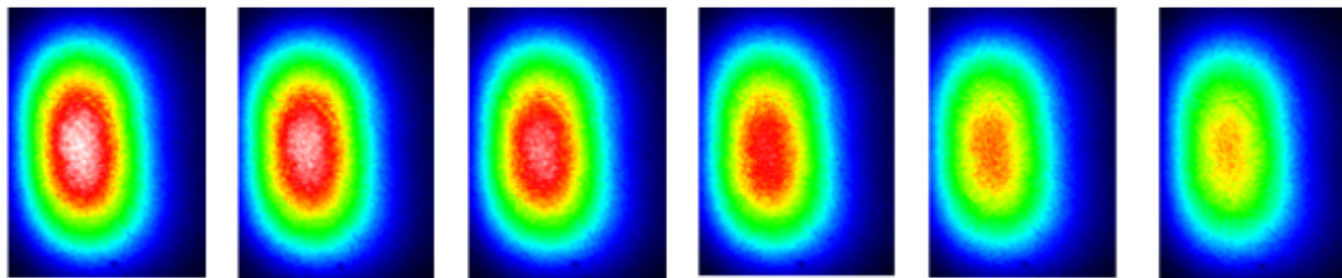
# Characterization of Combustion Instability



$\Phi=0.50$  0.46 0.42 0.38 0.34 0.30 0.26 0.22

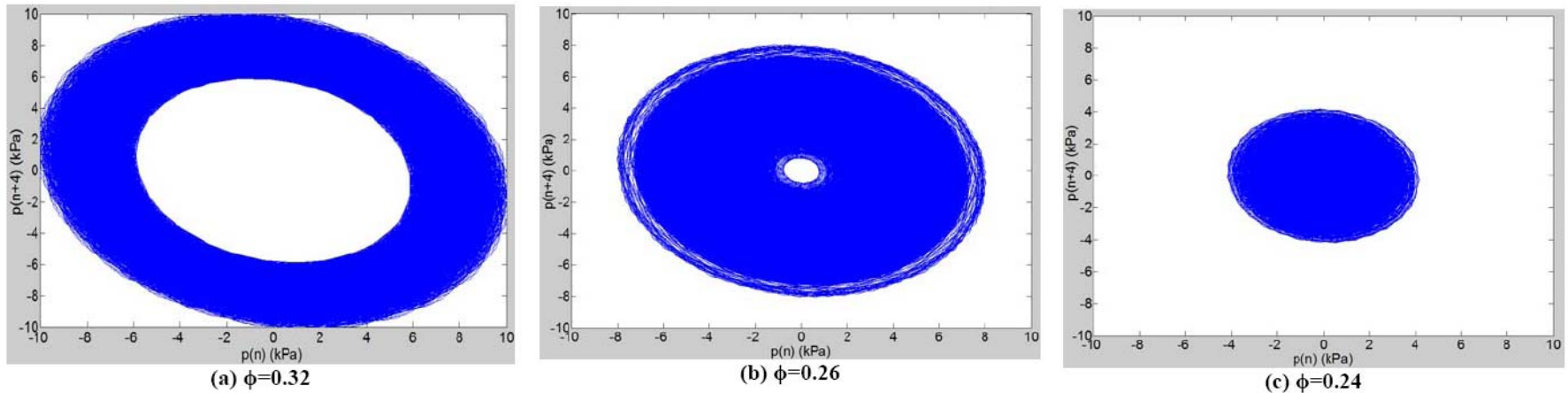


86° 116° 146° 176° 206° 236° 266°

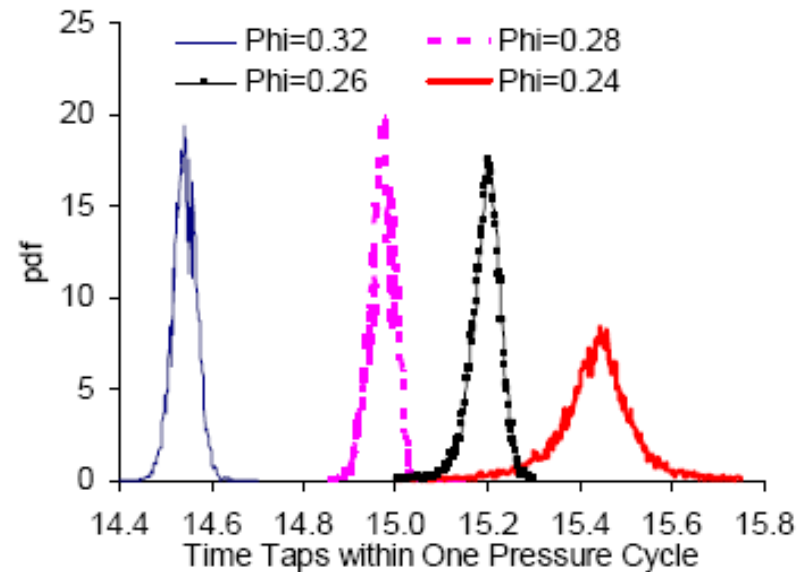
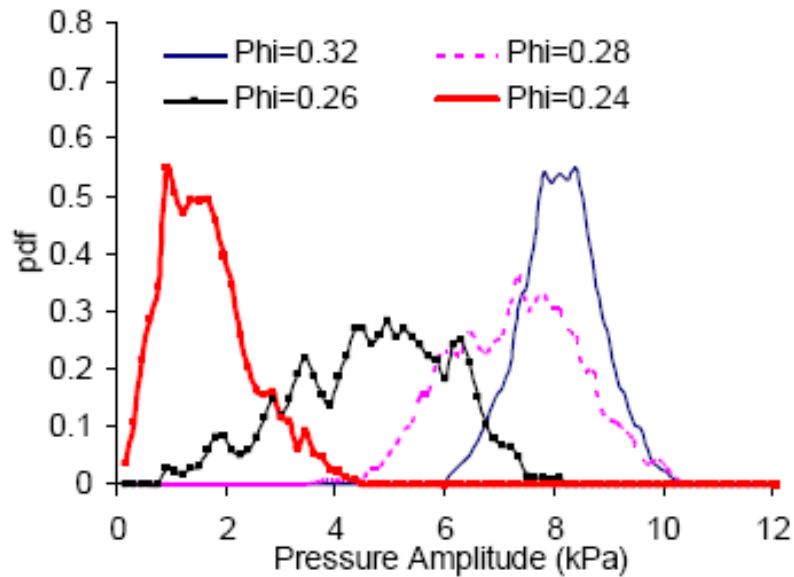


296° 326° 356° 386° 416° 446°

# Characterization of Combustion Instability (Cont.)



Phase Portrait of Self-Excited Combustion Instability



Probability Density Function of Pressure Amplitude and Period

# 5. Conclusions and Suggested Future Work



NASA Award No: NNX07C98A

# Conclusions

- Performed systematic investigations of flame response to fuel modulations up to 1 kHz and to air modulations up to 900 Hz.
- Developed strategies for accurate determination of the instantaneous heat release rate and equivalence ratios, which take into account of the nonlinearity among heat release, chemiluminescence, equivalence ratios, and acoustics-induced chemiluminescence oscillations.
- Proposed that a single adaptive robust controller be used for simultaneously control of both combustion instability and lean blowout.

# Suggested Future Work

- Development of high-frequency fuel-modulation technologies
- Quantification of flame response within a large range of working conditions
- Implementation of combustion control experiments



# Reference

1. T. Yi and D. A. Santavicca, "Flame Spectra for Turbulent Liquid-Fueled Swirl-Stabilized LDI Combustion," *Journal of Propulsion and Power*, Vol.25, No.5, pp.1058-1067, 2009.
2. T. Yi and D. A. Santavicca, "Forced Flame Response of Turbulent Liquid-Fueled Swirl-Stabilized LDI Combustion to Fuel Modulations," *Journal of Propulsion and Power*, Vol.25, No.6, pp.1259-1271, 2009.
3. T. Yi and D. A. Santavicca, "Combustion Instability in a Turbulent Liquid-Fueled Swirl-Stabilized LDI Combustion," under review at *Journal of Propulsion and Power* (similar to AIAA2009-5014).
4. T. Yi and D. A. Santavicca, "Determination of Instantaneous Fuel Flow Rates out of a Fuel Injector," *ASME Journal of Engineering for Gas Turbines and Power*, Vol.132, No.2, 2010.
5. T. Yi and D. A. Santavicca, "Flame Transfer Functions for Turbulent Liquid-Fueled Swirl-Stabilized LDI Combustion," *ASME Journal of Engineering for Gas Turbines and Power*, Vol.132, No.2, 2010.
6. T. Yi and E. J. Gutmark, "Stability and Control of Lean Blowout in Chemical-Kinetics-Controlled Combustion Systems," *Combust. Sci. and Technol.*, Vol.181, No.2, pp.226-244, 2009.
7. T. Yi and E. J. Gutmark, "Adaptive Control of Combustion Instability Based on Dominant Acoustic Modes Reconstruction," *Combust. Sci. and Technol.*, Vol.180, No.2, pp.249-263, 2008.
8. T. Yi and E. J. Gutmark, "Online Prediction of the Onset of Combustion Instability based on the Computation of Damping Ratios," *Journal of Sound and Vibration*, Vol.310, No.1-2, pp.442-447, 2008.
9. T. Yi and E. J. Gutmark, "Real-Time Prediction of Incipient Lean Blowout in Gas Turbine Combustors," *AIAA Journal*, Vol.45, No.7, pp.1734-1739, 2008.
10. T. Yi and E. J. Gutmark, "Dynamics of a High Frequency Fuel Actuator and its Applications for Combustion Instability Control," *ASME J. Eng. Gas Turbines Power*, Vol.129, pp. 648-654, 2007.
11. D. Wee, T. Yi, A. M. Annaswamy, and A. F. Ghoniem, "Self-Sustained Oscillations and Vortex Shedding in Backward-Facing Step Flows: Simulation and Linear Instability Analysis," *Physics of Fluids*, Vol. 16, No. 9, pp. 3361-3373, 2004.
12. T. Yi, D. Wee, A. M. Annaswamy, and A. F. Ghoniem, "Self-Sustained Oscillations in Separating Flows I: Stability Analysis and Reduced-Order Modeling," *Proceedings of the International Symposium on Combustion Noise and Control*, pp. 214-220, Cranfield University, 2003.
13. T. Yi, A. M. Annaswamy, and A. F. Ghoniem, "Self-Sustained Oscillations in Separating Flows II: Reduced-Order Modeling and Control," *Proceedings of the International Symposium on Combustion Noise and Control*, pp. 221-227, Cranfield University, 2003.



***Thanks !***



**NASA Award No: NNX07C98A**